Control of mode/bond selectivity and product energy disposal by the transition state: The X + H_2O (X=H, F, O(^{3}P), and Cl) reactions

Bin Jiang and Hua Guo*

Department of Chemistry and Chemical Biology, University of New Mexico, Albuquerque, New Mexico 87131

Supporting Information

S-I. Quantum Scattering Theory

The integral cross sections (ICS) for the atom-triatom reactions are calculated using the Chebyshev real wave packet (CRWP) method.[1-2] The CRWP method for atom-diatom reactions has been discussed in detail elsewhere,[3-5] we therefore focus here on its application to atom-triatom reactions. The six-dimensional Hamiltonian ($\hbar = 1$) can be written in the ABC+D Jacobi coordinates (see Fig. S-1):

$$\hat{H} = -\frac{1}{2\mu_1}\frac{\partial^2}{\partial r_1^2} - \frac{1}{2\mu_2}\frac{\partial^2}{\partial r_2^2} - \frac{1}{2\mu_3}\frac{\partial^2}{\partial r_3^2} + \frac{\hat{j}_1^2}{2\mu_1 r_1^2} + \frac{\left(\hat{j}_{12} - \hat{j}_1\right)^2}{2\mu_2 r_2^2} + \frac{\left(\hat{J} - \hat{j}_{12}\right)^2}{2\mu_3 r_3^2} + V\left(r_1, r_2, r_3, \theta_1, \theta_2, \varphi\right), \tag{1}$$

where the r_1 is the bond length of AB bond, r_2 the distance between the centre of mass of AB and C, and r_3 the distance between D and the centre of mass of triatomic molecule ABC. μ_i (i=1, 2, 3) are the corresponding reduced masses, $\hat{j}_1$, $\hat{j}_{12}$, and $\hat{J}$ are the angular momentum operators for AB, ABC and total system, respectively.

We choose to work in the body-fixed (BF) frame in which the z' axis lies along the r_3 vector and r_2 is in the $x'z'$ plane. The BF frame is related to the space-fixed (SF) frame (xyz) *via* a rotation defined by three Euler angles. The projection of the total angular momentum J onto the SF or BF frame is given by M or K. For convenience, we define a molecular-fixed (MF) frame in which the z'' axis lies along r_2 vector and r_1 is in the $x''z''$ plane. Note that the BF and MF frames for atom–triatom system (ABC+D) are equivalent to the SF and BF frames respectively for the atom-diatom subsystem (ABC). As a result, the projection of the j_{12} onto the BF or MF frame is given by K or m, and m is also the projection of j_1 onto the MF frame.

The overall rotational basis used in this work is the so-called primitive or uncoupled angular basis,[6-7] which has the following parity-adapted form:

$$\left|j_{12}j_1Km:JMp\right\rangle=\sqrt{\frac{1}{2(1+\delta_{K0}\delta_{m0})}} \times\left[\left|JMK\right\rangle\left|j_{12}j_1Km\right\rangle+p(-1)^J\left|JM-K\right\rangle\left|j_{12}j_1-K-m\right\rangle\right], \tag{2}$$

where $p=\pm1$ is the parity, $\left|JMK\right\rangle$ is the normalized Wigner rotational matrix defined in terms of the Euler angles,[8]

$$\left|JMK\right\rangle=\sqrt{\frac{2J+1}{8\pi^2}}D^{J\ *}_{MK}(\alpha,\beta,0), \tag{3}$$

and $\left|j_{12}j_1Km\right\rangle$ is, on the other hand, the angular basis of ABC in the MF frame (namely the BF frame for ABC itself),[9]

$$\left|j_{12}j_1Km\right\rangle=D^{j_{12}}_{Km}(0,\theta_2,\varphi)y_{j_1m}(\theta_1,0)=d^{j_{12}}_{Km}(\theta_2)e^{im\varphi}y_{j_1m}(\theta_1,0), \tag{4}$$

where $d^{j_{12}}_{Km}(\theta_2)$, $e^{im\varphi}$, and $y_{j_1m}(\theta_1,0)$ represent the reduced Wigner matrix, exponential Fourier function, and the spherical harmonic function, respectively.

This uncoupled angular basis $\left|j_{12}j_1Km:JMp\right\rangle$ is different from the coupled angular basis $\left|j_{12}j_1Kl_2:JMp\right\rangle$ used by other authors,[10] who have adapted a triatomic angular basis $\left|j_{12}j_1Kl_2\right\rangle$ in the BF frame (namely the SF frame for ABC), where l_2 is the orbital momentum of AB with respect to C. However, the uncoupled basis is related with the coupled one through a transformation,[9]

$$
\begin{aligned}
&\left| j_{12} j_1 K l_2 : JMp \right\rangle \\
&= \sqrt{\frac{1}{2(1+\delta_{K0})}} \times \left[\left| JMK \right\rangle \left| j_{12} j_1 K l_2 \right\rangle + p(-1)^{J+j_{12}+j_1+l_2} \left| JM-K \right\rangle \left| j_{12} j_1 -K l_2 \right\rangle \right] \\
&= \sum_m \sqrt{\frac{(1+\delta_{K0}\delta_{m0})}{(1+\delta_{K0})}} C_{j_2 m} \left| j_{12} j_1 K m : JMp \right\rangle,
\end{aligned}
\tag{5}
$$

where $C_{l_2 m} = \sqrt{(2l_2+1)/(2j_{12}+1)} \left\langle j_1 m l_2 0 \middle| j_{12} m \right\rangle$ is the Clebsch–Gordan coefficient.[8] Similar to the diatom-diatom system,[6] the uncoupled basis is advantageous for transformation back and forth between a grid and basis representation when computing the action of the potential energy operator. We refer the readers to earlier publications[6-7,10-11] for more details.

The action of angular kinetic energy operators (KEOs) on this rotational basis give rise to a diagonal or tridiagonal form,

$$
\frac{\hat{j}_1^{\,2}}{2\mu_{r_1} r_1^{\,2}} \left| j_{12} j_1 K m : JMp \right\rangle = \frac{j_1 \times (j_1+1)}{2\mu_{r_1} r_1^{\,2}} \left| j_{12} j_1 K m : JMp \right\rangle, \tag{6}
$$

$$
\begin{aligned}
&\frac{\left(\hat{j}_{12} - \hat{j}_1\right)^2}{2\mu_1 r_2^{\,2}} \left| j_{12} j_1 K m : JMp \right\rangle \\
&= \frac{j_{12} \times (j_{12}+1) + j_1 \times (j_1+1) - 2m^2}{2\mu_1 r_2^{\,2}} \left| j_{12} j_1 K m : JMp \right\rangle \\
&- \frac{\lambda^+_{j_{12} m} \lambda^+_{j_1 m} \sqrt{1+\delta_{K0}\delta_{m0}} \left| j_{12} j_1 K, m+1 : JMp \right\rangle + \lambda^-_{j_{12} m} \lambda^-_{j_1 m} \sqrt{1+\delta_{K0}\delta_{m1}} \left| j_{12} j_1 K, m-1 : JMp \right\rangle}{2\mu_1 r_2^{\,2}},
\end{aligned}
\tag{7}
$$

$$
\begin{aligned}
&\frac{\left(\hat{J} - \hat{j}_{12}\right)^2}{2\mu_3 r_3^{\,2}} \left| j_{12} j_1 K m : JMp \right\rangle \\
&= \frac{J(J+1) + j_{12}(j_{12}+1) - 2K^2}{2\mu_3 r_3^{\,2}} \left| j_{12} j_1 K m : JMp \right\rangle \\
&- \frac{\lambda^+_{JK} \lambda^+_{j_{12} K} \sqrt{1+\delta_{K0}\delta_{m0}} \left| j_{12} j_1 K+1, m : JMp \right\rangle + \lambda^-_{JK} \lambda^-_{j_{12} K} \sqrt{1+\delta_{K1}\delta_{m0}} \left| j_{12} j_1 K-1, m : JMp \right\rangle}{2\mu_3 r_3^{\,2}},
\end{aligned}
\tag{8}
$$

where the quantity $\lambda_{ab}^{\pm} = \sqrt{a(a+1) - b(b \pm 1)}$.

The action of the potential energy operator is evaluated in the discrete variable representation (DVR), which is a direct product of the Gauss-Legendre quadrature points in θ_1 and θ_2, and a Fourier grid in φ.[12-13] The transformation matrix between the angular basis and the DVR is consist of three one-dimensional pseudo-spectral transformations,[14]

$$U_{j_1 i_1}^{m} = \sqrt{\omega_{i_1}}\, y_{j_1 m}(\theta_{i_1}, 0), \tag{9}$$

$$U_{j_{12} i_2}^{Km} = \sqrt{\omega_{i_2}}\, d_{Km}^{j_{12}}(\theta_{i_2}), \tag{10}$$

$$U_{m i_3} = \sqrt{\omega_{i_3}}\, e^{im\varphi_{i_3}}, \tag{11}$$

where ω_{i_1} , ω_{i_2} and ω_{i_3} are corresponding quadrature weights and θ_{i_1} , θ_{i_2} and φ_{i_3} are corresponding quadrature roots. In particular, taking advantage of the inversion symmetry of the potential, only a sine (cosine) function only for odd (even) parity is needed when K equals 0.[12] While for K>0, which is indeed required in the exact close-coupling (CC) calculation, Eq. (11) can be expanded as both sine and cosine functions, resulting in two separate blocks in the vector-matrix multiplication and both contributing to one calculation of a specific parity.[7] This allows us to perform the wavepacket propagation in a real domain, so that significant memory savings can be achieved comparing to a complex wavepacket propagation. On the other hand, sine-DVR[15] was used for the two reactive radial degrees of freedom r_3 and r_2 typically and potential optimized DVR (PODVR)[16] was used for r_1 while it is non-reactive. For reactions that both channels are open, sine-DVR was used for all radial coordinates.

The initial wave packet $|\Psi_i\rangle$ was defined in the space-fixed (SF) representation with a direct product of the ro-vibrational eigenfunction $|\psi_{v_i, j_{12i}}\rangle$ of the triatom and a Gaussian wave packet in the scattering coordinate:[4]

$$|\Psi_i\rangle = Ne^{-(R-R_0)^2/2\delta^2} \cos k_0 R |\psi_{v_i, j_{12i}}\rangle |j_{12i} l_{12i}, Jp\rangle, \tag{12}$$

where N is the normalization factor, R_0 and δ the mean position and width of the Gaussian function, j_{12i} and l_{12i} are the initial total angular momentum of ABC and the initial orbital angular momentum of ABC with respect to D, l_{12i} is determined by $|J - j_{12i}| \le l_{12i} \le |J + j_{12i}|$. The mean momentum k_0 is related to the mean kinetic energy E_0 *via* $k_0 = \sqrt{2\mu_R E_0}$. This SF initial wave function was converted to the BF frame before propagation.

The wave packet propagation was implemented using the modified three-term Chebyshev iteration,[17-19]

$$|\Psi_k\rangle = 2D\hat{H}_s |\Psi_{k-1}\rangle - D^2 |\Psi_{k-2}\rangle, \qquad k \ge 2, \tag{13}$$

where $|\Psi_1\rangle = D\hat{H}_s |\Psi_0\rangle$ and $|\Psi_0\rangle = |\Psi_i\rangle$. D is a damping function defined in the edges of the grid to impose outgoing boundary conditions,[17]

$$D(\zeta) = \begin{cases} 1 & \zeta < \zeta_d, \\ e^{-\alpha\left(\frac{\zeta - \zeta_d}{\zeta_{\max} - \zeta_d}\right)^2} & \zeta \ge \zeta_d, \end{cases} \tag{14}$$

where $\zeta = r_3$, r_2, or r_1. The scaled Hamiltonian is defined as:

$$\hat{H}_s = (\hat{H} - \bar{H}) / \Delta H, \tag{15}$$

to avoid the divergence of the Chebyshev propagator outside the range [-1, 1]. Here, the mean and half-width of the Hamiltonian are determined as $\bar{H} = (H_{\max} + H_{\min})/2$ and $\Delta H = (H_{\max} - H_{\min})/2$, where $H_{\max}$ and $H_{\min}$ define the spectral range of the Hamiltonian and can be estimated from the kinetic and potential energies on the grid.

The initial state-selected reaction probability was obtained directly by analyzing the flux through the dividing surface in the product channel ($r = r_f$),[3]

$$P^J_{v_i, j_{12i}, l_{12i}}(E_c) = \frac{1}{2\pi\mu_r \left|a_i(E_c)\right|^2 \Delta H^2 (1 - E_s^2)} \times \\ \mathrm{Im}\left[\left\langle \sum_{k=0} (2 - \delta_{k0}) e^{-ik \arccos E_s} \Psi_k \right| \times \delta(r - r_f) \frac{\partial}{\partial r} \left| \sum_{k'=0} (2 - \delta_{k'0}) e^{-ik' \arccos E_s} \Psi_{k'} \right\rangle \right]_{r=r_f}, \tag{16}$$

where E_c is the collision energy, E_s the scaled energy ($E_s = (E - \bar{H})/\Delta H$), $a_i(E_c)$ the energy amplitude of the initial wave packet, and the dividing surface could be set up in either r_1 or r_2.

The initial state-specified integral cross section (ICS) can then be obtained by summing initial state-specified reaction probabilities ($P^J_{v_i, j_{12i}, l_{12i}}(E_c)$) over all contributing partial waves

$$\sigma_{v_i, j_{12i}}(E_c) = \frac{1}{2 j_{12i} + 1} \sum_{l_{12i}} \left\{ \frac{\pi}{2\mu_{r_3} E_c} \sum_J (2J + 1) P^J_{v_i, j_{12i}, l_{12i}}(E_c) \right\}. \tag{17}$$

Both the CC and centrifugal sudden (CS)[20-21] calculations have been performed. To verify our method, calculations for the H + H_2O reaction have been performed for several *J* values at both CC and CS levels and the results compare well with the earlier results of Zhang et al.[22] In Fig. S-2, the comparison between CC and CS results are presented for both the F + H_2O and O + H_2O reactions. The numerical parameters used in our CRWP calculations are given in Table S-I.

Table S-I. Numerical parameters used in calculations on three PESs. (Atomic units are used unless stated otherwise.)

Parameters	$H+H_2O$[a]	$F+H_2O$	$O+H_2O$
Grid/basis ranges and sizes	$r_3 \in [1.4,\ 14.0]$ $N_{r_3}^{\text{tot}} = 72,\ N_{r_3}^{\text{int}} = 25$ $r_2 \in [1.0,\ 5.0]$ $N_{r_2}^{\text{tot}} = 28,\ N_{r_2}^{\text{int}} = 8$ r_1=1.865 $(N_{\theta 1}, N_{\theta 2}, N_\varphi)$ = (15, 30, 15)	$r_3 \in [2.0,\ 18.0]$ $N_{r_3}^{\text{tot}} = 220,\ N_{r_3}^{\text{int}} = 58$ $r_2 \in [1.0,\ 5.0]$ $N_{r_2}^{\text{tot}} = 25,\ N_{r_2}^{\text{int}} = 7$ $r_1 \in [1.2,\ 5.0]$, $N_{\text{PODVR}} = 7$ $(N_{\theta 1}, N_{\theta 2}, N_\varphi)$ = (18, 38, 18)	$r_3 \in [2.0,\ 14.0]$ $N_{r_3}^{\text{tot}} = 220,\ N_{r_3}^{\text{int}} = 60$ $r_2 \in [1.0,\ 5.0]$ $N_{r_2}^{\text{tot}} = 25,\ N_{r_2}^{\text{int}} = 5$ $r_1 \in [1.0,\ 4.0]$, $N_{\text{PODVR}} = 4$ $(N_{\theta 1}, N_{\theta 2}, N_\varphi)$ = (18, 35, 18)
Absorbing potential	For r_3: ζ_d=10.5, α=0.1 For r_2: ζ_d=3.2, α=0.1	For r_3: ζ_d=16.0, α=0.1 For r_2: ζ_d=3.2, α=0.1 For r_1: ζ_d=2.4, α=0.1	For r_3: ζ_d=12.0, α=0.1 For r_2: ζ_d=3.0, α=0.1
Initial wavepacket	$R_0 = 10.0, \delta = 0.40$ E_0 = 1.00 eV	$R_0 = 15.8, \delta = 0.15$ E_0 = 0.25 eV	$R_0 = 11.5, \delta = 0.10$ E_0 = 1.00 eV
Flux position	$r_{2\text{flux}}$=2.9	$r_{2\text{flux}}$=3.1	$r_{2\text{flux}}$=2.8
Converged $J_{\max}$		120	150/170
Propagation step	1000	7000	2000

[a]: Parameters used for comparison with Ref. 22

Fig. S-1. The atom-triatom Jacobi coordinates used in the quantum scattering calculations.

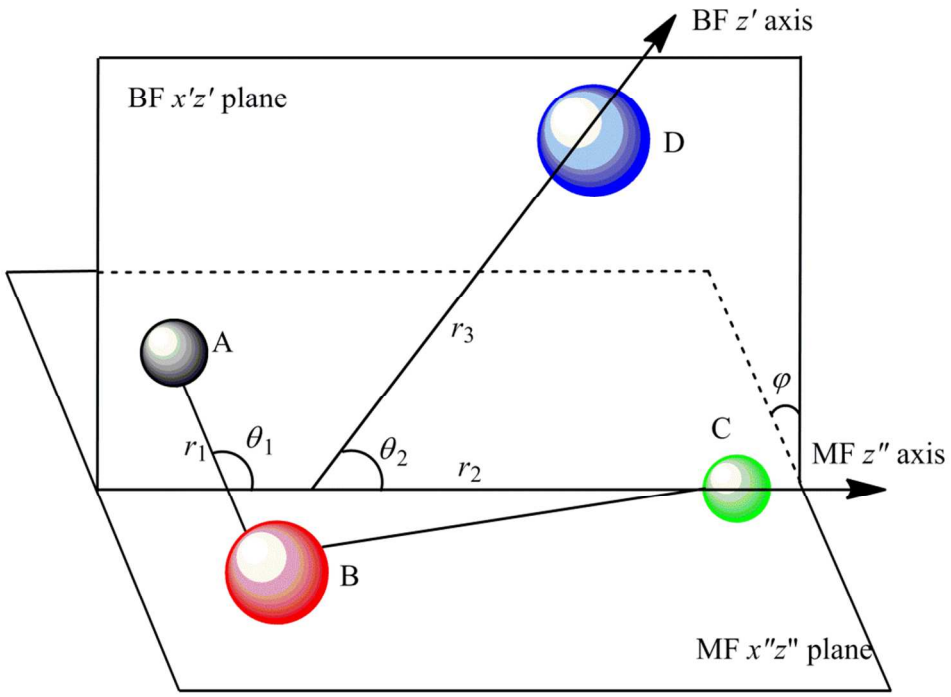

Fig. S-2 Top panel: Comparison of the CC and CS ICSs for the F + H_2O(000) reaction. Lower panel: Comparison of the CC and CS reaction probabilities for the O + H_2O(000) reactions at several *J* values.

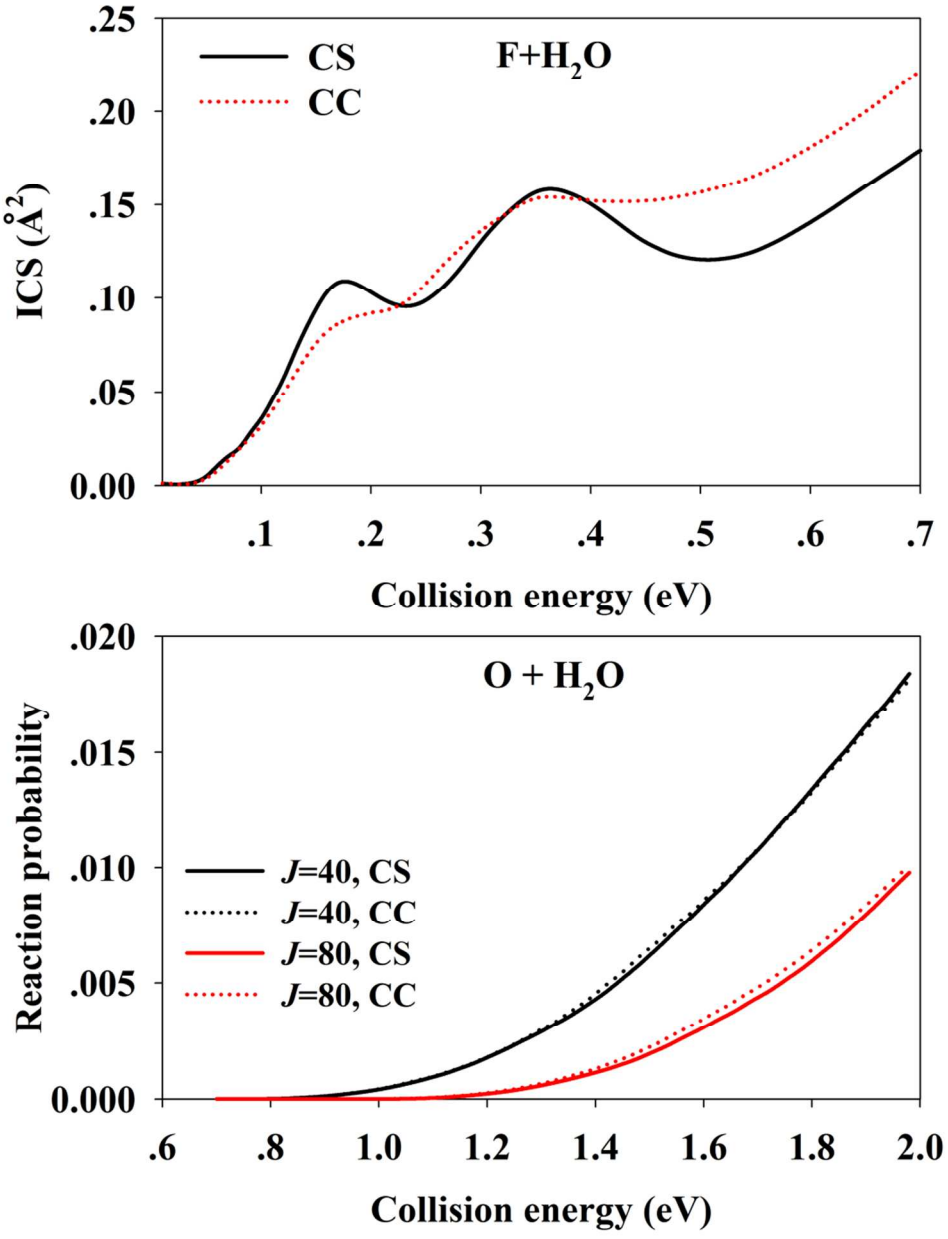

References:

(1) Goldfield, E. M.; Gray, S. K. *Adv. Chem. Phys.* **2007**, *136*, 1.
(2) Guo, H. *Int. Rev. Phys. Chem.* **2012**, *31*, 1.
(3) Lin, S. Y.; Guo, H. *J. Chem. Phys.* **2003**, *119*, 11602.
(4) Lin, S. Y.; Guo, H. *Phys. Rev. A* **2006**, *74*, 022703.
(5) Ma, J.; Lin, S. Y.; Guo, H.; Sun, Z.; Zhang, D. H.; Xie, D. *J. Chem. Phys.* **2010**, *133*, 054302.
(6) Chen, R.; Ma, G.; Guo, H. *J. Chem. Phys.* **2001**, *114*, 4763.
(7) Goldfield, E. M.; Gray, S. K. *J. Chem. Phys.* **2002**, *117*, 1604.
(8) Zare, R. N. *Angular Momentum*; Wiley: New York, 1988.
(9) Zhang, J. Z. H. *Theory and Application of Quantum Molecular Dynamics*; World Scientific: Singapore, 1999.
(10) Zhang, D. H.; Light, J. C. *J. Chem. Phys.* **1996**, *104*, 4544.
(11) Lin, S. Y.; Guo, H. *J. Chem. Phys.* **2002**, *117*, 5183.
(12) Yu, H.-G.; Muckerman, J. T. *J. Molec. Spectrosc.* **2002**, *214*, 11.
(13) Jiang, B.; Xie, D.; Guo, H. *J. Chem. Phys.* **2011**, *135*, 084112.
(14) Corey, G. C.; Tromp, J. W.; Lemoine, D. In *Numerical Grid Methods and Their Applications to Schroedinger's Equation*; Cerjan, C., Ed.; Kluwer: Dordrecht, 1993, p 1.
(15) Colbert, D. T.; Miller, W. H. *J. Chem. Phys.* **1992**, *96*, 1982.
(16) Echave, J.; Clary, D. C. *Chem. Phys. Lett.* **1992**, *190*, 225.
(17) Mandelshtam, V. A.; Taylor, H. S. *J. Chem. Phys.* **1995**, *103*, 2903.
(18) Chen, R.; Guo, H. *J. Chem. Phys.* **1998**, *108*, 6068.
(19) Gray, S. K.; Balint-Kurti, G. G. *J. Chem. Phys.* **1998**, *108*, 950.
(20) Pack, R. T. *J. Chem. Phys.* **1974**, *60*, 633.
(21) McGuire, P.; Kouri, D. J. *J. Chem. Phys.* **1974**, *60*, 2488.
(22) Zhang, D. H.; Yang, M.; Lee, S.-Y. *J. Chem. Phys.* **2002**, *117*, 10067.
(23) Fu, B.; Zhang, D. H. *J. Chem. Phys* **2013**, *138*, 184308.